THE JOURNAL OF BIOLOGICAL CHEMISTRY
Vol. 275, No. 12, Issue of March 24, pp. 8582–8591, 2000
© 2000 by The American Society for Biochemistry and Molecular Biology, Inc.
Printed in U.S.A.

Unusual Oxidative Chemistry of N^{ω}-Hydroxyarginine and *N*-Hydroxyguanidine Catalyzed at an Engineered Cavity in a Heme Peroxidase*

(Received for publication, September 24, 1999, and in revised form, December 8, 1999)

Judy Hirst‡ and David B. Goodin§

From the Department of Molecular Biology, Scripps Research Institute, La Jolla, California 92037

Heme enzymes are capable of catalyzing a range of oxidative chemistry with high specificity, depending on the surrounding protein environment. We describe here a reaction catalyzed by a mutant of cytochrome *c* peroxidase, which is similar but distinct from those catalyzed by nitric-oxide synthase. In the R48A mutant, an expanded water-filled cavity was created above the distal heme face. *N*-Hydroxyguanidine (NHG) but not guanidine was shown to bind in the cavity with K_d = 8.5 mM, and coordinate to the heme to give a low spin state. Reaction of R48A with peroxide produced a Fe(IV)=O/Trp$^{\cdot+}$ center capable of oxidizing either NHG or N^{ω}-hydroxyarginine (NHA), but not arginine or guanidine, by a multi-turnover catalytic process. Oxidation of either NHG or NHA by R48A did not result in the accumulation of NO, NO_2^-, NO_3^-, urea, or citrulline, but instead afforded a yellow product with absorption maxima of 257 and 400 nm. Mass spectrometry of the derivatized NHA products identified the yellow species as *N*-nitrosoarginine. We suggest that a nitrosylating agent, possibly derived from HNO, is produced by the oxidation of one molecule of substrate. This then reacts with a second substrate molecule to form the observed *N*-nitroso products. This complex chemistry illustrates how the active sites of enzymes such as nitric-oxide synthase may serve to prevent alternative reactions from occurring, in addition to enabling those desired.

Heme enzymes catalyze oxidative reactions by either electron or hydrogen atom abstraction, or by oxygen transfer. These basic chemistries, when combined with steric and electronic control over the access of substrates to the oxidizing center, result in an enormous range of highly specific reactions, which include radical-based oxidations (peroxidases) (1, 2) and epoxidation or hydroxylation of olefins and aromatic compounds (P_{450}) (3), as well as complex mixed-function oxidase/oxygenase reactions (prostaglandin synthase, nitric-oxide synthase) (4). The role of the protein environment in controlling the reaction pathway for a given enzyme is often discussed in terms of how a specific reaction is enabled. Two examples of this in heme enzymes are the push-pull hypothesis and the substrate access principle. In the push-pull hypothesis (5–7), specific protein active site groups, including the proximal axial heme ligand and distal polarizing amino acid side chains, participate in facilitating the cleavage of the Fe^{3+}-OOH peroxy bond to produce a ferryl (Fe^{4+}=O) center (with or without associated radical species). This highly reactive (~1 V) species is capable of either the abstraction of an electron or hydrogen atom from substrate, or the insertion of an oxygen atom. The type of chemistry that actually occurs is often predominantly controlled by how substrate molecules are allowed to gain access to this oxidizing center. Substrates held at some distance, for example near the heme edge, are limited to sequential one-electron oxidation reactions typified by the peroxidases (3, 8). Substrates that are positioned adjacent to the reactive Fe^{4+}=O oxygen group above the distal heme face can participate in oxo-transfer chemistry via concerted or oxygen rebound mechanisms (4, 9). Much less, however, is known about the almost certain need for these enzymes to evolve reaction pathways that avoid the occurrence of alternative chemistries; these may result, for example, from the improperly controlled release of partially oxidized intermediates or from the incorrect positioning of substrates near the ferryl oxygen. This is partially due to the fact that, despite a large body of work on model porphyrin compounds (10–12), the limits of the reactions available to a ferryl heme in the context of a protein active site are still being discovered.

A significant example of our developing knowledge of the reactions catalyzed by oxidized heme centers is the enzymatic oxidation of arginine by nitric-oxide synthase (NOS),[1] to produce nitric oxide (NO) (13, 14). This five-electron oxidation proceeds in two steps: an initial two-electron oxidation to form N^{ω}-hydroxyarginine (NHA) followed by a three-electron oxidation to release citrulline and NO (Table I) (15–18). In the normal enzymatic cycle, both reactions require O_2 and reducing equivalents from NADPH, and are believed to involve the heme and/or H_4B in oxidative chemistry that shares some features with that of P_{450} enzymes and peroxidases. When H_2O_2 is used instead of NADPH/O_2, NOS is unable to carry out the initial hydroxylation of arginine but will oxidize NHA to generate alternative products. In this case, and also for H_4B-free en-

* This work was supported by a Wellcome Trust Prize International Research Fellowship to J. H and by National Institutes of Health Grant GM41049 (to D. B. G.). The costs of publication of this article were defrayed in part by the payment of page charges. This article must therefore be hereby marked "*advertisement*" in accordance with 18 U.S.C. Section 1734 solely to indicate this fact.

The atomic coordinates and structure factors (codes 1DJ1 and 1DJ5) have been deposited in the Protein Data Bank, Research Collaboratory for Structural Bioinformatics, Rutgers University, New Brunswick, NJ (http://www.rcsb.org/).

‡ Supported by a Wellcome Trust Prize International Research Fellowship. Current address: Medical Research Council, Dunn Human Nutrition Unit, Hills Rd. Cambridge, CB2 2XY, UK.

§ To whom correspondence should be addressed: Dept. of Molecular Biology, MB8, Scripps Research Inst., 10550 N. Torrey Pines Rd., La Jolla, CA 92037. Tel.: 858-784-9892; Fax: 858-784-2857; E-mail: dbg@scripps.edu.

[1] The abbreviations used are: NOS, nitric-oxide synthase; CCP, cytochrome *c* peroxidase; CCP(MKT), cytochrome *c* peroxidase produced by expression in *Escherichia coli* containing Met-Lys-Thr at the N terminus, Ile at position 53, and Gly at position 152; CN-orn, N^{δ}-cyanoornithine; ES-MS, electrospray ionization-mass spectrometry; MPD, 2-methyl-2,4-pentanediol; NHA, N^{ω}-hydroxyarginine; NHG, *N*-hydroxyguanidine; WT, wild type CCP; HPLC, high performance liquid chromatography; GC-MS, gas chromatography-mass spectrometry.

This paper is available on line at http://www.jbc.org

TABLE I
Functional groups of relevant chemical species

functional group	R=$(CH_2)_3NHCH(NH_2)COOH$	R=H
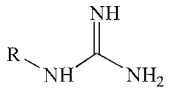	arginine	guanidine
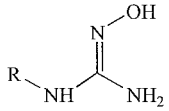	N^{ω}-hydroxyarginine	N-hydroxyguanidine
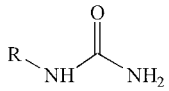	citrulline	urea
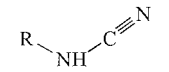	N^{δ}-cyanoornithine	cyanamide
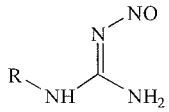	N-nitrosoarginine	N-nitrosoguanidine
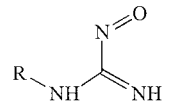	nitrosoamidine intermediate	
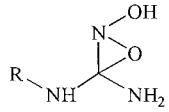	oxyaziridine intermediate	

zyme, HNO and a mixture of citrulline and N^{δ}-cyano-ornithine (CN-orn) are produced (19–21). These results clearly illustrate the importance of correctly coupling the redox equivalents in order to avoid alternative chemistry and to determine a specific course of reaction.

For these reasons, it is important to determine in greater detail the inherent specificity of the oxidation reactions of guanidine compounds, positioned near a ferryl heme within a protein matrix. One approach that is often successful is chemical rescue or cavity complementation, in which the deletion of an amino acid side chain in a protein produces a cavity capable of binding compounds of complementary properties, thus allowing the functional properties of the recruited compound to be evaluated. This somewhat crude approach has worked in a surprising number of cases including amine rescue of lysine deletions (22), metal-ligand replacement in several metalloproteins (23–25), and electron transfer from compounds bound at the former site of a redox-active amino acid free-radical (26, 27). Here, we describe the structural and functional properties of the R48A cavity mutant of cytochrome *c* peroxidase (CCP), in which a binding site for guanidine compounds has been created on the distal face of the heme. Arg-48 lies within 4 Å of the heme in the distal active site cleft, and assists the heterolytic cleavage of the ferric peroxy O-O bond during enzyme turnover (6). Compounds bound to the R48A cavity are oxidized by the ferryl heme in reactions that are similar to, but clearly distinct from those of NOS, other heme enzymes or chemical agents. These results thus help to further extend our understanding of the diverse oxidative chemistry that may occur between substrates positioned near reactive heme centers in enzymes.

EXPERIMENTAL PROCEDURES

CCP Expression and Purification—The R48A mutant of CCP was constructed by site-directed mutagenesis of pT7CCP using the QuikChange site-directed mutagenesis kit (Stratagene) and was overexpressed in *Escherichia coli* BL21(DE3). Both the R48A mutant and wild-type CCP(MKT) were purified as described previously (26). Nitrophorin-1 was expressed and purified from *E. coli* according to previously published procedures (46).

Spectrometry and Kinetic Measurements—UV-visible absorption spectra were collected at 20 °C using a Hewlett-Packard 8453 diode-array spectrometer. For binding titrations, a solution of ~10 μM protein was equilibrated in the cuvette in 100 mM phosphate, pH 6.0, for 20 min and the spectrometer blanked. Difference spectra were then recorded at equilibrium, following the addition of small aliquots of concentrated stock solutions of ligand (1 M), also corrected to pH 6. Dissociation constants and cooperativity were evaluated using Scatchard and Hill plots. Kinetic spectrometric measurements were conducted using an OLIS RSM-1000 rapid scanning stopped-flow spectrometer. Solutions of protein (final concentration: 2–5 μM)/substrate/H_2O_2 were prepared in 100 mM phosphate buffer at pH 6 and equilibrated to temperature in the spectrometer prior to reaction; data were evaluated either using the OLIS fitting software, or by numerical (digital) simulation. Errors for rate constant measurements are estimated to be ±5%.

X-ray Crystallography—Single crystals of R48A were grown overnight, at 18 °C, from sitting drops of 10% 2-methyl-2,4-pentanediol (MPD), 40–60 mM potassium phosphate (pH 6.0), and 0.17 mM R48A and were soaked in 25% MPD as cryoprotectant before flash-freezing in a liquid nitrogen cryostream for data collection. For structures containing bound ligand, the MPD solution additionally contained 10 mM hydroxyguanidine (corrected to pH 6.0) and crystals were soaked for 20 min prior to freezing. X-ray diffraction data were collected at 100 K using CuKα radiation from the rotating anode of a Siemens SRA x-ray generator and Siemens area detector. Data were processed using the XENGEN package (28) and analyzed by difference Fourier techniques using the XtalView software (29). Molecular replacement using the AMoRe package (30) was used to compensate for small differences in the unit cell observed as a result of freezing, and refinement of the structure was done using repeated cycles of manual adjustment and Shelxl97 (31).

Ion-pair High Performance Liquid Chromatography (HPLC)—Guanidine and hydroxyguanidine could be individually observed using ion-pair HPLC on a C_{18} column (LC18, Supelcosil), running isocratically at 1 ml min^{-1}. The solvent mixture was filtered and sparged with helium before use, comprised 90% 25 mM HOAc/NaOAc, pH 4.35, and 10% MeOH and contained 15 mM hexane sulfonic acid (Aldrich), as the ion-pairing reagent (32). Prior to analysis, protein was removed from the reaction mixture by ultrafiltration (Centricon-30), and the solution composition and pH corrected to correspond to the HPLC running buffer. As determined by standard solutions, the response was linear for concentrations up to at least 10 mM, loaded in 20-μl aliquots.

Amino Acid Derivatization and Analysis—Amino acid derivatization and analysis was performed using the following methods: (i) HPLC, according to the Waters AccQTag Method (Waters Chromatography) and (ii) mass spectrometric analysis. Amino acids were derivatized by phenylisothiocyanate (PITC) as follows (33, 34); 25 nmol of sample was dissolved into 8 μl of H_2O, 8 μl of ethanol, and 4 μl of triethylamine and re-dried under vacuum. The residue was then redissolved into 20 μl of the derivatization mixture (7:1:1:1 mixture of ethanol:H_2O:triethylamine:PITC, respectively) and the reaction allowed to proceed for 20 min at room temperature, before re-drying under vacuum to remove excess reagents. The derivatized amino acids were purified, and all salts removed, by reversed phase HPLC using a C_{18} column. Solvent A comprised H_2O with 0.1% trifluoroacetic acid, and solvent B contained 90% acetonitrile, 10% H_2O, and 0.09% trifluoroacetic acid. The derivatized amino acids discussed here eluted at between 20 and 30% solvent B. Fractions from the HPLC were collected and immediately analyzed using a Sciex API-III triple quadrupole (electrospray) mass spectrometer, equipped with an ion-spray atmospheric pressure ionization source. Samples were injected using a syringe infusion pump at 5 μl min^{-1} coupled directly to the ionization source by a fused silica capillary of 100 μm internal diameter, and ionized at a positive potential of 4700 V and an orifice potential of 70 V. Spectra were acquired by scanning quadruple 1 from m/z 200–800 Da with a scan step of 0.1, and recorded and processed using the Tune and Mac Spec (PE-Sciex) programs on a Macintosh computer.

Nuclear Magnetic Resonance (NMR) and Infrared Spectroscopy

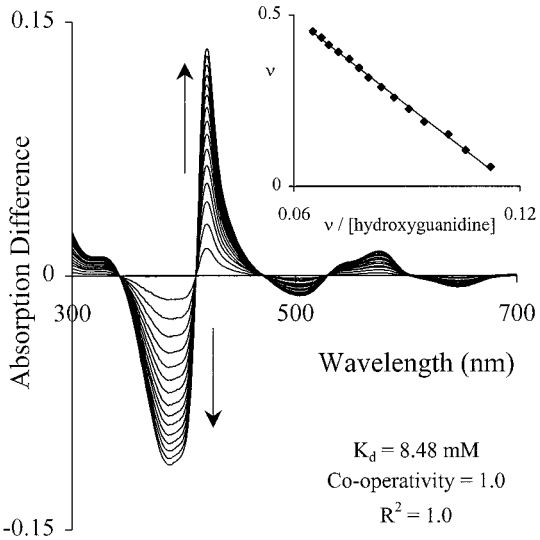

FIG. 1. ***N*-Hydroxyguanidine binding to R48A.** Optical difference spectra for R48A (10 μM) in 100 mM phosphate, pH 6.0, volume 2 ml, titrated with successive additions of 2 μl of 1 M NHG (corrected to pH 6.0) at 20 °C. Spectral changes occurred immediately. Before titration commenced, 10 μM NHG was added to the R48A solution and equilibrated for 30 min. This corrected a small change in the spectrum which was also observed for WT enzyme. *Inset*, Scatchard plot, corresponding to the data presented in the main figure.

(IR)—Samples for NMR and IR analysis were lyophilized overnight prior to experimentation, to remove water and NH_4OAc buffer. NMR samples were then dissolved in dry d_6-dimethyl sulfoxide (d_6-Me_2SO, Cambridge Isotopes Inc.) containing a particle of molecular sieve (4 Å) to remove traces of water. All spectra (^1H at 600 MHz and ^{13}C at 151 MHz) were recorded on a DRX 600 Bruker spectrometer, and referenced to the ^{13}C or ^2D signal of the d_6-Me_2SO as appropriate. IR spectra were recorded as a KBr powder using a Perkin Elmer FT-IR Paragon 1000 PC spectrometer.

NO Analysis—The Griess reaction assay (colorimetric nitric oxide assay kit, Calbiochem) was used to analyze for nitrite and nitrate (35), the breakdown products of NO and NO^- under aerobic conditions (19). For nitrate analysis, nitrate reductase and NADH were first added and incubated at room temperature for 20 min to reduce all the nitrate to nitrite. The two Griess reagents (sulfanilamide and napthylethylenediamine) were then added and the total concentration of nitrite evaluated by measuring the final absorbance of the Griess reaction adduct at 540 nm. The linearity of the response was established by using standard solutions. Direct measurements of NO production during turnover were also made in anaerobic solutions using an NO electrode (ISO-NOP, World Precision Instruments) standardized using a saturated solution of NO.

Urea Analysis—Concentrations of urea were measured using a commercial urea analysis kit (Raichem, San Diego, CA); urease is used to convert urea to ammonia and the concentration of urea calculated via formation of a colored ammonia adduct. The response was linear for concentrations up to 5 mM, in the experimentally relevant buffer solution.

RESULTS

Binding of Hydroxyguanidine to R48A—The R48A mutant of CCP was constructed to introduce a potential binding site for guanidine and its derivatives near the heme active site. Arg-48 is in the distal heme pocket and is proposed to aid the heterolytic cleavage of the iron-bound peroxy bond during reaction with H_2O_2 (6, 36, 37). Many studies have exploited the combination of amino acid side-chain deletion with "chemical rescue" (22) or "cavity complementation" (23–27, 38, 39) whereby function is restored or induced by the addition of complementary ligands. We thus considered that guanidine compounds, bound in the R48A cavity in close proximity to the heme center, would be in a prime position for oxidation. While titration of both R48A and WT CCP with guanidine or arginine resulted in only small, non-saturating changes in the spectrum, Fig. 1 shows that addition of NHG to a 10 μM solution of R48A mutant induced a dramatic change in the optical spectrum of the enzyme; the progressive change upon titration can be accurately assigned to binding of NHG with K_d = 8.48 mM, as shown by the Scatchard plot inset to Fig. 1. The red shift observed in the heme Soret region, along with decreased intensity of the charge-transfer bands at 507 and 645 nm and the appearance of bands at 540 and 574 nm, are all indicative of conversion of the high spin ferric heme to a low spin state. In addition, the five isosbestic points at 342, 410, 472, 529, and 604 nm clearly indicate a two-state conversion upon binding. The spin-state alteration implies a change in coordination, suggesting that NHG binds directly to the heme iron. Additions of NHG to wild-type (WT) CCP did not result in significant changes in the spectra, indicating that the Arg-48 side chain precludes binding. Thus, we conclude that the R48A mutant has acquired the ability to bind NHG at the heme center, utilizing the cavity created by deletion of Arg-48.

TABLE II
X-ray data collection and refinement statistics

Data collection	R48A	R48A-NHG
a (Å)	105.5	105.0
b (Å)	74.3	73.8
c (Å)	44.3	43.8
Resolution (Å)	2.00	1.93
I/σ_I (av)	12.4	18.1
I/σ_I (last shell)	2.2	3.1
Unique reflections	23,101	23,476
Completeness (%)	84.0	85.8
R_{sym}	6.6	6.7
Refinement		
R_{cryst}	0.16	0.16
Resolution (Å)	1.93	1.93
No. of reflections	22,135	22,720
r.m.s.$_{bond}$ (Å)[a]	0.006	0.006
r.m.s.$_{angle}$ (deg)	1.75	1.68
No. of waters	487	409

[a] r.m.s., root mean square.

Structure Determination of R48A with and without Bound NHG—Replacement of Arg-48 with alanine results in an expanded, water-filled cavity on the distal heme face. The R48A crystal structure was determined at 2.0 Å resolution (100 K, Table II) and compared with WT CCP at a resolution of 1.8 Å (room temperature, Protein Data Bank entry 1cca) (40). No significant changes were observed outside the immediate vicinity of the deleted Arg-48 side chain. In the active site region (Fig. 2*A*), a small change was observed in the His-52 side-chain plane, resulting principally from a ~25° rotation about the C_β-Cγ bond. The three water molecules (W313, W344, and W300), which are observed adjacent to Arg-48 in the distal active-site cavity of WT CCP, remain in R48A but have shifted by 0.3, 0.5, and 0.4 Å, respectively, from their positions in WT enzyme. The expanded cavity in R48A is structurally well defined and incorporates three additional well ordered solvent molecules (W394, W423, and W514) that are not observed in WT CCP. The position of NHG bound to R48A was obtained by soaking a crystal in 10 mM hydroxyguanidine for 20 min prior to freezing. The data was refined against a model that did not include the ligand, in order to compute the $F_o - F_c$ omit map shown in Fig. 2*B*. This map, contoured at 3 and 4 σ, shows a clearly defined, planar, trefoil-shaped electron density feature above the heme, which is roughly the size and shape expected for the NHG molecule, except that the position of the hydroxyl group was not evident. It is clear from Fig. 2*B* that the bound NHG would be sterically excluded from WT CCP by the Arg-48 side chain, verifying that the binding capacity is enabled by cavity complementation. The NHG molecule is not, however, positioned directly over the missing guanidinium group of WT

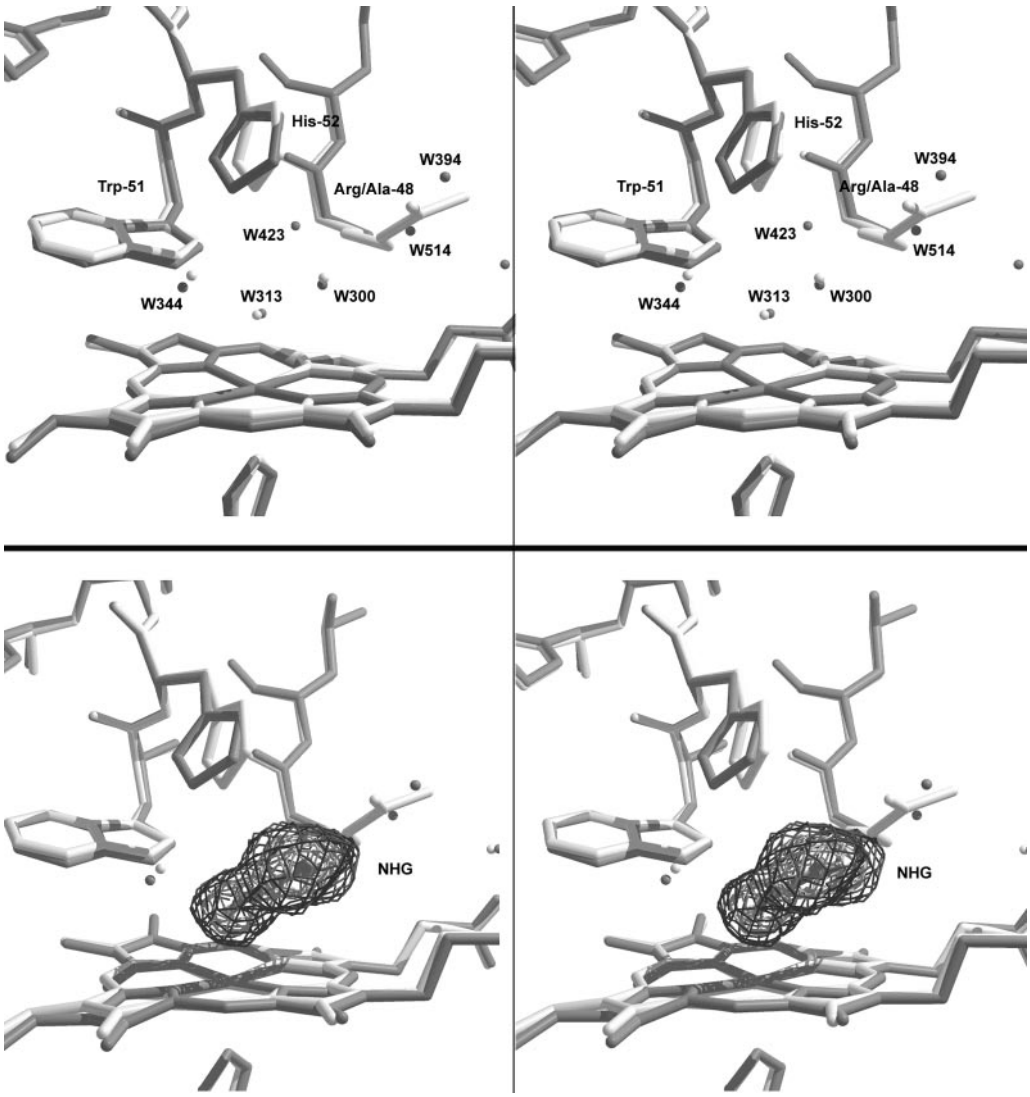

FIG. 2. **X-ray crystallographic characterization of R48A.** *A*, *(Top)*, comparison of the structures of WT CCP (*light color*, Protein Data Bank 1cca, room temperature, 1.8 Å) and R48A (*dark color*, 100 K, 1.93 Å). The structure is conserved throughout except in the immediate vicinity of the mutation, where a small change in the orientation of the side chain of His-52 has occurred, and three new ordered water molecules (W394, W423, and W514) have been incorporated into the R48A cavity. *B*, (*Bottom*), NHG substrate bound in the R48A cavity. The R48A structure determined with the bound ligand (*dark color*, 100 K, 1.93 Å) is superimposed upon the structure of WT CCP (*light color*). The bound ligand density is shown as the $F_o - F_c$ omit map, contoured at 3 and 4 σ.

R48 but instead has one of its trefoil density lobes directly over the heme iron. This leaves two of the R48A cavity waters (W394 and W514) in place, but displaces R48A cavity water W423, as well as two of the waters that are observed in WT CCP (W300 and W313). Unambiguous orientation of the NHG ligand was not possible due to the apparent symmetry of the electron density feature; the orientation chosen places the hydroxyl group at ~1.8 Å from the heme iron, serving as a coordinating ligand as is consistent with the high to low spin conversion upon binding, and also accounting for the angle between the ligand and heme planes (41, 42). With this placement, two hydrogen bonds are observed between the two guanidine nitrogens (-NH_2 groups) and W514 and W368.

Absence of Chemical Rescue in R48A—Since the Arg-48 side chain plays an important role in cleaving the O-O bond during reaction of the ferric enzyme with H_2O_2 (6), guanidine was examined for its ability to repair the functional lesion created by the R48A mutation. Consistent with previously studied Arg-48 mutants (36, 37), the rate of compound I formation for R48A (1.33 μM^{-1} s^{-1}) is impaired relative to WT CCP (37.3 μM^{-1} s^{-1}), as measured by stopped-flow experiments in which ferric enzyme (2.5 μM) was reacted with varying amounts of peroxide (10–50 μM). However, experiments conducted in the presence of guanidine displayed no change in rate. Thus, the decreased rate of reaction of the ferric enzyme with H_2O_2 is not recovered by guanidine complementation, consistent with the indication above that guanidine does not interact with R48A.

Catalytic Oxidation of N-Hydroxyguanidine and N^{ω}-Hydroxyarginine—R48A catalyzed the peroxide-induced oxidation of NHA and NHG, but not of arginine or guanidine. Initial experiments compared the ability of these four potential substrates to react with the peroxide-induced ferryl heme state. Upon addition of one equivalent of H_2O_2 to a solution containing 5 μM R48A, the optical spectrum (λ_{max} = 418 nm; α, β bands at 530 and 560 nm) characteristic of a ferryl heme was observed, and persisted for at least 10 s without visible decay; this persistence of the oxidized heme was unaffected by the presence of arginine or guanidine. However, when NHA or NHG were present, no ferryl state was observable using a standard spectrophotometer and thus was either not formed or reacted completely before the spectrum could be recorded (~2 s). Further experiments showed that these substrates were not merely inhibiting the

reaction of the enzyme with H_2O_2, as addition of 5 μM WT CCP to a solution in which 5 μM R48A had previously been reacted with 100 μM H_2O_2, in the presence of 1 mM amounts of either NHA or NHG, did not result in the oxidation of the WT enzyme, indicating that at least 20 equivalents of peroxide had been consumed by catalytic turnover of R48A. This reactivity was specific to the R48A mutant, as experiments with WT CCP showed that the peroxide-induced compound I state was unreactive toward all four substrates.

Hydroxyguanidine Oxidation Kinetics—R48A catalyzed the oxidation of NHG at significantly enhanced rates with respect to WT CCP. Wild-type CCP compound I is stable enough to allow transfer into the stopped-flow spectrometer, and temperature equilibration before reaction; thus, its reaction with NHG could easily be quantified. A very slow reaction was observed, which returned compound I to the ferric state but required several seconds even in 25 mM NHG and which displayed a second-order rate constant of 2.82×10^{-5} μM^{-1} s^{-1}. R48A compound I was not stable enough for transfer and equilibration in the stopped-flow spectrometer, complicating quantification of the kinetics; this relative instability of compound I is a common feature among mutants of CCP. The evolution of the ratio of ferric to ferryl species during turnover (in solutions containing both H_2O_2 and NHG) was therefore used to evaluate the rate of the reaction. Three kinetic regimes were apparent, depending on the relative amounts of H_2O_2 and NHG added. (i) In a large excess of NHG, the ferric spectrum remained unperturbed - each ferryl center formed reacts immediately. (ii) In a small concentration of NHG, the majority of the R48A was held in the ferryl state, until all the H_2O_2 was consumed and the system returned to the ferric state. (iii) In the intermediate regime, a steady-state ratio of ferric and ferryl enzyme was quickly established, which again reverted to all-ferric after total consumption of the H_2O_2. The amount of H_2O_2 present was limited experimentally by the need to avoid oxidative damage to the enzyme. Typical experimental results are presented in Fig. 3*A*. The ratio of [Fe^{3+}] to [Fe^{4+}=O] was determined from the relative intensity of the Soret band at 418 nm, where the difference in the two spectra was most apparent. The rate of reaction between compound I and NHG was then calculated using a finite difference procedure to simulate the varying amounts of each species present, according to Scheme I. An excellent fit was obtained over a large range of experimental conditions (up to 200 μM H_2O_2 and 1 mM NHG); an example is shown in Fig. 3*B*. Most importantly, the rate of reaction of R48A compound I with NHG is 0.28 μM^{-1} s^{-1}: 10,000 times faster than that of WT compound I; a direct comparison of measured rate constants is shown in Fig. 4. Furthermore, the rate of compound I formation is slightly increased from its value in the absence of NHG (1.33 to 2.50 μM^{-1} s^{-1}), perhaps indicating the effect of an NHG molecule transiently bound in the Arg-48 pocket, in close proximity to the heme center.

Chromatographic Analysis of Oxidation Products—Reversed-phase HPLC using a C_{18} column and hexanesulfonic acid as ion-pairing agent (32) provided a rapid and direct observation of NHG consumption in the reaction with R48A. Standard curves showed that the amount of NHG injected onto the column was accurately reflected by the area of the elution peak, monitored at 200 nm. As shown by the ion-pair HPLC traces in Fig. 5*A*, NHG was completely converted upon reaction to a separate product peak, which is likely to consist of multiple unresolved species (see below), due to the low resolution and retention time of the ion-pair column. Consumption of NHG by the reaction was used to determine the NHG:H_2O_2 stoichiometry. Separate aliquots of 5 mM NHG in 25 mM acetate buffer at pH 6.0 were reacted with varying amounts of H_2O_2 in the presence of ~10 μM R48A. The reaction was followed spectrophotometrically to ensure the heme returned to the ferric state after the reaction was complete, for cases in which NHG was in excess. Samples of the reaction mixture were then analyzed by ion-pair HPLC for the quantity of remaining NHG. The results, shown in Fig. 6, indicated that one H_2O_2 molecule is required for each NHG consumed.

Ion-pair HPLC also provided preliminary characterization of the crude product fraction that was produced by oxidation of either NHG or NHA. The product peak, isolated following the reaction of either substrate, was distinctly yellow in color, with

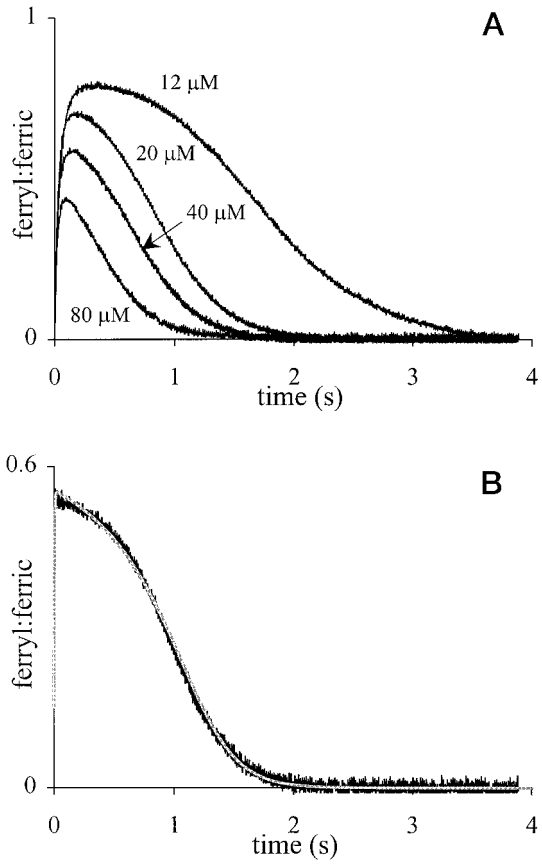

FIG. 3. **Catalytic turnover of 2 μM R48A in 9 μM peroxide and varying amounts of *N*-hydroxyguanidine, showing evolution of the ratio of ferryl and ferric enzyme, as calculated from the absorption at 418 nm.** *A*, at a high concentration of NHG, the concentration of ferryl species remains low as the ferryl state is most rapidly re-reduced by NHG. At lower concentrations, more R48A is maintained in the oxidized state during turnover. In every case, NHG is present in excess; the enzyme thus ultimately returns to the ferric state. All experiments in 100 mM phosphate buffer, pH 6.0, 20 °C. In *B* is a comparison of experimental and modeled data for a typical kinetic trace. Conditions were as follows: 2 μM R48A, 100 μM H_2O_2, 389 μM hydroxyguanidine. Rate constants: k_1 = 2.50 μM^{-1} s^{-1}, k_2 = 0.28 μM^{-1} s^{-1}, as defined in Scheme I.

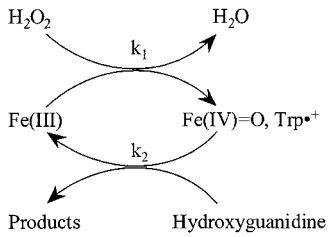

SCHEME 1. **Turnover of R48A.** Reaction of ferric enzyme with hydrogen peroxide produces compound I, which is then reduced by two electrons by *N*-hydroxyguanine.

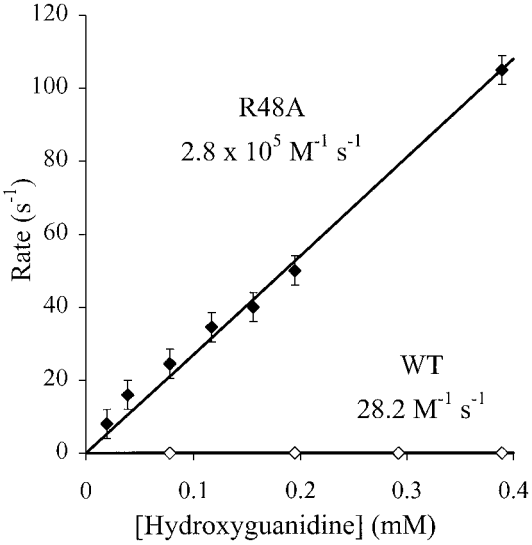

FIG. 4. **Comparison of rates of reaction between the ferryl state in R48A and WT CCP with NHG.** The R48A rates were deduced from the reaction profiles modeled as shown in Fig. 3, and WT data are from stopped-flow measurements of the reaction of ferryl enzyme with *N*-hydroxyguanidine in 100 mM phosphate buffer, pH 6.0, 20 °C.

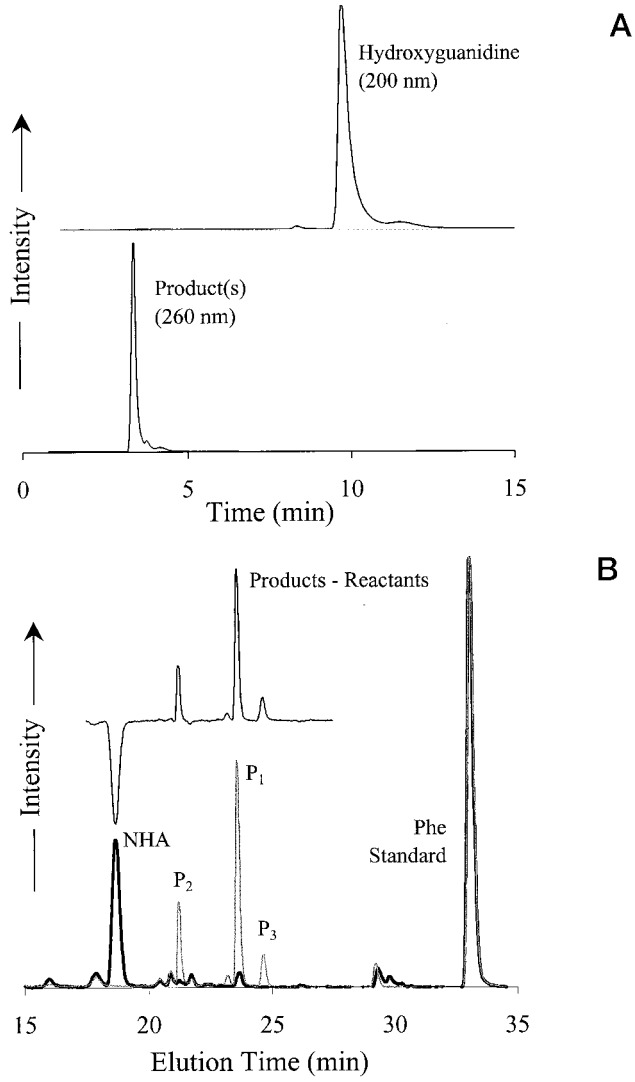

FIG. 5. **HPLC analysis of R48A reaction products.** In *A*, ion-pair HPLC traces showing elution of *N*-hydroxyguanidine (*upper trace*, monitored at 200 nm), and of the product mixture from the stoichiometric reaction of peroxide and NHG, catalyzed by R48A (*lower trace*, monitored at 260 nm). Both traces are normalized in intensity. Enzyme was removed from the product mixture by ultrafiltration (Centricon-30), and the composition and pH of each sample corrected prior to chromatography. The second, small product peak at a slightly greater elution time increased if excess peroxide was added to the reaction mixture. Conditions for HPLC: C_{18} column, isocratic gradient of 90% 25 mM HOAc, pH 4.35, 10% methanol, 15 mM hexanesulfonic acid, 1 ml min^{-1}. *B*, HPLC traces of AccQTag amino acids analyzed using the Waters chromatography system. The *dark trace* shows the reactant, dominated by elution of N^{ω}-hydroxyarginine at ~18 min and also by a signal from Phe at ~34 min, which was added to the reaction mixture before reaction to allow direct comparison of the amounts of material present in the reactant and product traces. The *lighter trace* shows elution of the products. The *single trace* at the *top* shows the difference between products and reactants, clearly defining the disappearance of N^{ω}-hydroxyarginine and the appearance of three new product species.

UV-visible absorption spectra (Fig. 7) exhibiting peaks at 257 nm and at 400 nm. The quantity of the products increased linearly with the quantity of NHG reacted, but the color of the isolated fraction was observed to decay on the bench over a period of several days. Similar experiments showed that guanidine was not converted under these conditions, and that both R48A and peroxide were necessary for the consumption of NHG. No conversion was observed in reactions with WT enzyme.

Higher resolution HPLC methods were used to demonstrate that R48A/H_2O_2 catalyzed the conversion of NHA into one major and two minor product species. It was found that the crude ion-pair HPLC product peak from NHA oxidation gave a positive ninhydrin test, demonstrating that the N-terminal amino functionality of the amino acid remained. This allowed high resolution HPLC analysis of the reaction products, following derivatization of the amino acid functionality using the Waters AccQTag method. It is clear from these results (Fig. 5*B*) that the single prominent peak of the reactant, NHA, is absent following reaction, and that three clear product peaks (labeled P_1, P_2, and P_3) are produced. In Fig. 5*B*, the relative scale of the product and reaction HPLC profiles have been normalized by the response of an internal phenylalanine standard, and the change in sample composition is thus shown more clearly by the difference profile (*inset* to Fig. 5*B*).

Citrulline and Urea Analyses—Attempts were made to detect the presence of urea based products in the reactions of R48A since many of the heme systems that are capable of oxidizing guanidine derivatives, including NOS, produce the corresponding urea. It was clear from the amino acid analysis described above that citrulline was not one of the three products of NHA oxidation, since authentic samples of citrulline eluted clearly separated from any of the products. Additional experiments also served to rule out significant quantities of urea in the reaction products of NHG oxidation. Although chromatographic or mass spectroscopic detection of urea at low concentrations was impractical, direct analysis using an enzymatic urease assay gave no indication of the formation of urea; addition of the predicted quantity of urea to the samples tested gave positive results. In addition, NMR spectra of lyophilized product mixtures from NHG oxidation were not consistent with the formation of urea. ^1H spectra in dry d_6-Me_2SO showed no non-exchangeable resonances, and a single broad peak, at 7.6 or 7.5 ppm for the NHG reactant and its products, respectively, consistent with the presence of a single set of exchangeable N-H protons. However, upon addition of urea, an additional broad resonance became apparent at 5.4 ppm showing that the observed signals were distinct from urea. The ^{13}C NMR spectrum of the product mixture (Fig. 8), gave a single peak at 158.57 ppm, compared with 159.01 ppm for NHG or 159.59 ppm for urea. Again, upon addition of authentic samples of either NHG or urea to the product mixture, two distinct peaks

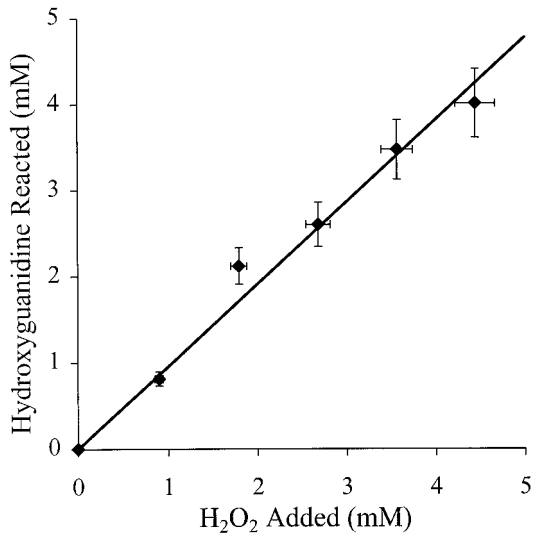

FIG. 6. **Determination of the stoichiometry for the reaction H_2O_2:NHG = 1:1.** A 5 mM stock solution of NHG was reacted with varying amount of H_2O_2 in the presence of R48A, and the amount of NHG remaining was determined using ion-pair chromatography as described in the text.

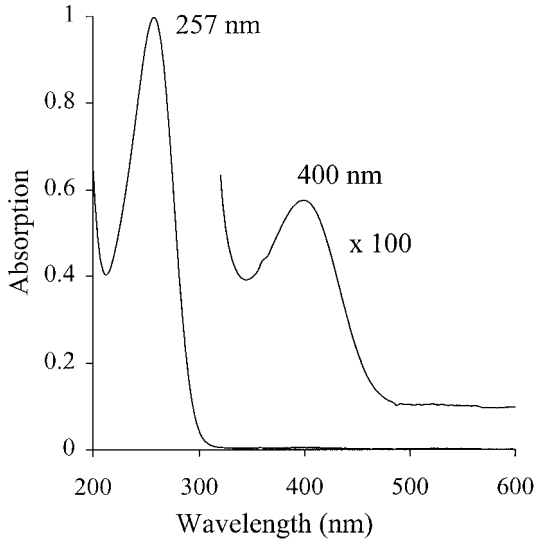

FIG. 7. **UV-visible spectra of the major product of NHG oxidation; the spectrum from NHA oxidation was very similar.**

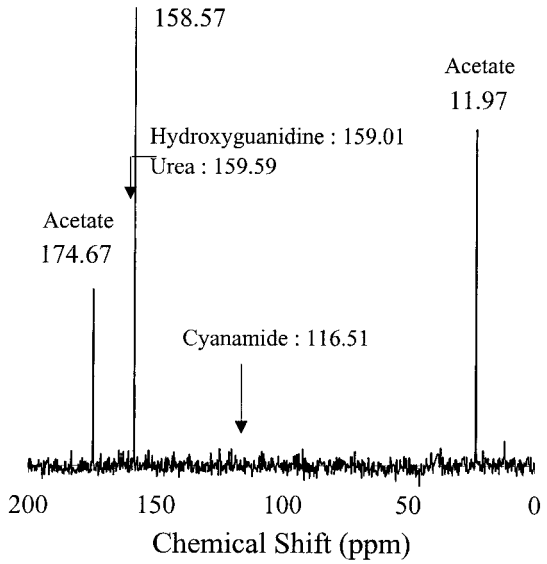

FIG. 8. **^{13}C NMR spectra of the non-volatile product(s) of *N*-hydroxyguanidine oxidation (after lyophilization), compared with those of urea and cyanamide.** Spectra were recorded at 151 MHz in d_6-Me_2SO and referenced to the solvent resonance DRX 600 Bruker spectrometer.

were observed. Finally, because it was necessary to lyophilize product samples prior to NMR analysis, any volatile components, such as cyanamide, would not be observed.

Analysis for NO_x Species—Several methods were used to analyze for the possible accumulation of nitrogen oxides. Under aerobic conditions, any NO or HNO produced would rapidly decompose and is typically detected as nitrite or nitrate by the Griess reaction (35). Total product mixtures of NHG or NHA oxidation by R48A gave positive Griess tests, and quantitative Griess assays of NHG oxidation products showed that one "nitrite equivalent" was produced for each peroxide molecule reacted. However, several lines of evidence forced the conclusion that this was not due to the accumulation of NO_x species. First, after isolation by ion-pair HPLC, the "product peak" (Fig. 5*A*) of NHG oxidation itself gave a positive Griess reaction. Second, co-injection of either nitrate, nitrite, or peroxynitrite (NO_x standards) with the product mixture showed that they eluted clearly separated from the product peak. No evidence for NO_x was observed in HPLC traces of the product mixture alone, and fractions of the product mixture collected at the retention times of NO_x standards gave negative Griess tests. Finally, approximately 1 min was taken for completion of the Griess reaction with NO_x standards, but approximately 20 min were required when the products of the NHG reaction were analyzed, indicating the detection of a different chemical entity. As the Griess reaction is known to occur with compounds other than nitrite, for example *N*-nitroso- or nitro- compounds (43, 44), it is possible that such a compound is producing our observed results.

Additional tests failed to detect the accumulation of NO_x species in reactions of R48A. Experiments using a nitric oxide electrode in sealed anaerobic reaction mixtures (50 μM R48A, 5 mM NHG, 2 mM H_2O_2) during steady-state turnover showed only small, transient responses upon initiation of the reaction, corresponding to less than 50 μM NO, which decayed back to base-line adducts within 15 s. The lifetime of the response was significantly shorter than that of an equivalent amount of NO injected into control samples, indicating that another species may be producing the response, or that any NO produced is also rapidly consumed by components of the reaction. Finally, it was not possible to detect various nitrosyl adducts that would be expected upon accumulation of NO; ferric R48A in the presence of NO would be expected to give rise to the ferric heme-NO complex, whereas in the presence of HNO the ferrous heme-NO (45) would result. UV-visible measurements on reaction mixtures during turnover failed to indicate the presence of the ferric- or ferrous-nitrosyl heme, while such species were easily observed upon addition of a known quantity of NO to the reaction. Furthermore, addition of ferric nitrophorin-1 (NP1) (46), which has a high affinity for NO also showed no evidence for NO or HNO formation; again, a positive result was readily obtained upon addition of a known sample of NO. Taken together, these experiments indicate that if NO or HNO is produced, it is rapidly consumed by further reactions that do not result in the appearance of nitrite, nitrate, peroxynitrite, or nitrosyl-heme adducts.

Identification of the Yellow Product—Further analysis of the reactions of NHG and NHA with R48A/H_2O_2 led to assignment of the yellow products as *N*-nitrosoguanidine and *N*-nitrosoarginine, respectively. Since the products of NHA oxidation retain their amino acid functionality, they can be derivatized

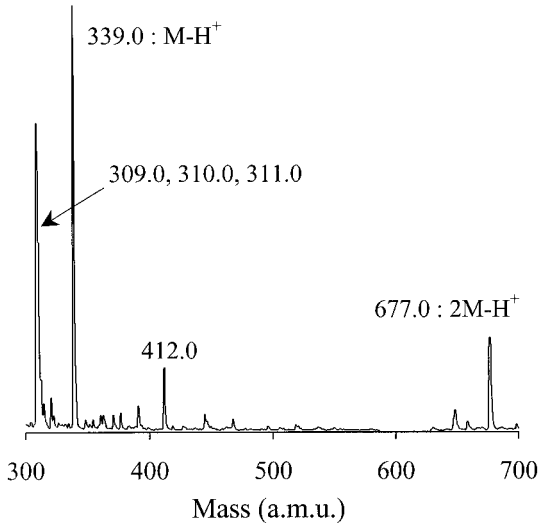

FIG. 9. **Mass spectra (positive-ion ES-MS) for one of the isolated PITC-derivatized products of the oxidation of N^{ω}-hydroxyarginine with H_2O_2, catalyzed by R48A.** NHA itself displays a single peak at 326 atomic mass units.

using PITC, isolated by C_{18} reverse-phase HPLC, and analyzed using positive ion electrospray mass-spectrometry (ES-MS). The PITC-derivatized NHA reactant was easily observed by ES-MS with a prominent peak at 326 atomic mass units and, as expected, was no longer present after reaction with R48A and H_2O_2. For the product mixture, at least one new PITC-derivatized species could be detected as shown in Fig. 9. This most prominent peak, at 339 atomic mass units, may be related to the peak at 677 atomic mass units by non-covalent dimer formation. Also present was a broader signal at around 310 atomic mass units, which could be resolved into three separate peaks at 309, 310, and 311 atomic mass units. Those at 310 and 311 may be assigned to small amounts of contaminating arginine or citrulline, which were also observed in samples of the NHA starting material and which co-elute with the product peak from the HPLC. Thus, the PITC-derivatized NHA product peak isolated by HPLC gives ES-MS spectra with prominent and novel peaks at 309, 339, and 667 atomic mass units, with the 339 atomic mass unit peak as the major species. 339 atomic mass units corresponds to an increase of 13 atomic mass units over PITC-derivatized NHA, and the peaks at 309 and 339 atomic mass units may be related by the loss of NO. As mentioned above, the 667-atomic mass unit peak is likely to be related to the 339-atomic mass unit peak by non-covalent dimerization. These data taken together suggest that the peak at 339 atomic mass units derives from PITC-derivatized *N*-nitrosoarginine (Table I), as it is the only reasonable chemical structure with this mass; it may easily lose NO to give rise to the 309-atomic mass unit peak, and nitroso compounds are also known to be prone to dimerization (47). In addition, no difference in the mass of any of these species was observed in reactions using $H_2{}^{18}O_2$, including the three peaks at 309, 310, and 311, indicating that no non-exchangeable oxygens in the product derive from H_2O_2 or the ferryl state of R48A. This assignment implies that *N*-nitrosoguanidine is the analogous product of NHG oxidation. This, in turn, is consistent with the NMR properties of the yellow product of NHG oxidation and with its UV-visible absorption characteristics (Fig. 7), which compare exactly with those of *N*-nitrosoguanidine (48). *N*-Nitrosoguanidine is also highly unstable explaining our repeated lack of success in identifying this species by mass-spectrometry (ES-MS, matrix-assisted laser desorption ionization, fast atom bombardment, and GC-MS). Finally, *N*-nitroso species such as these are known to give positive Griess reaction assays (43).

Other Organic Species—The identification of *N*-nitrosoguanidine(arginine) as one of the products implies that a second reaction product must also be formed, since the *N*-nitroso products have gained an additional nitrogen atom, which ultimately must have been derived from a second reactant molecule. Indeed, the derivatized products of the NHA reaction (Fig. 5*B*) show the presence of additional products. While we have been unable to identify these species in the mass-spectrometry experiments described above, by analogy with the known oxidative chemistry of *N*-hydroxyguanidine the missing fragment is likely to be CN-orn or cyanamide for the NHA and NHG reactions, respectively. Since cyanamide is volatile (with a boiling point of 89 °C), we would expect it to be lost upon lyophilization, and so its absence from the NMR spectra is not diagnostic. We have noted signals that correspond to the mass expected for cyanamide by GC-MS, although these experiments proved generally difficult and irreproducible. However, while the Fourier transform-infrared spectra of the lyophilized NHG product mixture was complex due to modes characteristic of RNH_2 and SO_4^{2-} (NHG obtained as the sulfate salt), a band at 2232 cm^{-1} could be observed in some samples, indicating the presence of cyanamide.

DISCUSSION

This study addresses a number of questions about the reactivity of a heme center in the context of reactions catalyzed by peroxidases, P_{450}, and NOS. In view of the recent structural studies of NOS (49, 50), in which the arginine substrate is observed to bind directly above the distal heme face, it is of interest to ask whether guanidine based compounds, placed in the distal heme cavity of a peroxidase will react with the ferryl heme. If so, how do the reactions compare with those of other heme enzymes? Finally, why isn't the arginine, ubiquitous in the distal active site of peroxidases (51), oxidized during turnover? Differences in the reactivity could be due to variations in the electronic structure of the heme, the details of the active site environment, the existence of other cofactors, or in the positioning of the substrate with respect to the ferryl center. On one hand, it is clear that the way in which substrates gain access to the ferryl center controls a significant part of the type of chemistry observed in heme enzymes. Indeed, several studies have demonstrated the engineering of novel oxidative reactions into peroxidases (27, 52, 53), P_{450} (54, 55), and Mb (56, 57) by manipulating the access of substrates to the oxidized heme. On the other hand, the details of the heme, cofactor, and amino acid environment of CCP (58), P_{450} (59), and NOS (15, 50, 60) contribute significantly to their unique activities. This paper attempts to address these issues by characterizing the reactions that result from positioning substrate analogs of a heme oxygenase, NOS, at the active site of a peroxidase, CCP.

Superficial similarities were observed between the reactivity of R48A and NOS. The expanded distal heme cavity created by the deletion of the Arg-48 side chain was shown to bind and oxidize NHG and NHA, but not arginine or guanidine. While it is possible that guanidine and arginine do not react because of the lack of binding to R48A, weak binding does not necessarily imply that these substrates do not have access to the heme; the *N*-hydroxyguanidine moiety may be inherently easier to oxidize than guanidine. In fact, this general trend is also observed for NOS operated by the peroxide shunt, when NHA but not arginine is oxidized (16). The initial oxidation of arginine to NHA by NOS is not well understood, and it is possible that cofactors such as the pterin, in addition to heme, are required to accomplish the initial hydroxylation. This conclusion may be more salient in view of the fact that the active-site arginine of peroxidases is not oxidized, despite extensive exposure to the

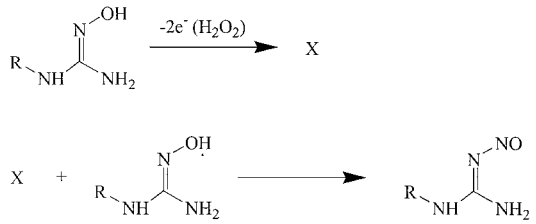

SCHEME II. Proposed mechanism for formation of the N-nitroso species.

ferryl heme center. Clearly, however, the similarities between R48A and NOS pale in light of the fact that different products are observed for the two enzymes, indicating that different mechanisms must operate.

The R48A/H_2O_2 catalyzed oxidation of NHG and NHA to produce the *N*-nitrosoguanidine product without the accumulation of NO, HNO, NO_2^-, NO_3^{2-}, or urea implies a different mechanism and different reaction intermediates from those observed in other heme enzymes. For CCP, the compound I intermediate produced upon reaction of the ferric enzyme with peroxide, contains a ferryl heme coupled to the Trp-191 cation radical (Fe^{4+}=O/$Trp^{+\bullet}$) (61). Compound I is produced extremely rapidly for peroxidases, and no ferric-peroxy intermediate has been observed. This state for CCP is also different from that of other peroxidases, in which a porphyrin cation radical is observed in place of the Trp-191 radical of CCP compound I. In either case, two oxidizing equivalents are stored as the formal equivalent of a ferrous iron bound to an oxygen atom and a second organic radical. For the currently accepted mechanism of NOS, the reactive intermediate, at least for the second oxidation step, is achieved by reduction of the ferrous-dioxygen complex (18). This should also generate a two-electron oxidized intermediate, formally equivalent to the compound I of peroxidases, except for two proposed differences. First, the bound NHA substrate itself is the proposed reductant in this reaction, leading to an NHA radical intermediate (16). In addition, the ferric-peroxy state has been proposed to persist, allowing the distal peroxy-oxygen to be transferred to the substrate in an electrophilic addition, and resulting in an overall three-electron oxidation of NHA to citrulline and NO (16). Clearly, these differences in the electronic nature of the reactive intermediates, between R48A/H_2O_2 and NOS/NADPH/O_2, would be expected to result in differing pathways for substrate oxidation. However, NOS will also operate with H_2O_2 (peroxide shunt) instead of NADPH/O_2 to convert NHA into a mixture of citrulline, CN-orn, and HNO (20). In this case, mechanisms were proposed that involved only the two-electron oxidized Fe^{4+}=O/$R^{\bullet}$ state reacting with NHA, to produce the observed products. In this respect, similar products might have been expected with the R48A system, and the different products that were observed suggest that storage of an oxidizing equivalent on the Trp-191 radical of CCP may be responsible.

Several proposals can be made concerning the novel products formed by the oxidation reactions of R48A. The quantitative conversion of NHG to *N*-nitrosoguanidine makes it necessary to transfer a nitrogen-containing moiety from one substrate to another, implying that two substrate molecules are used in the formation of each *N*-nitroso species. We postulate three alternative hypotheses. (i) The unique chemical nature of the compound I intermediate (Fe(IV)=O/$Trp^{\bullet+}$) may effectively separate the reaction into two one-electron oxidation reactions, with the formation of NHG radicals. Subsequent disproportionation reactions could result in the novel products observed. While this proposal could explain the 1:1 substrate:peroxide stoichiometry if one oxidation equivalent were lost at each step, such a bimolecular radical recombination reaction would be also expected to give very nonspecific product profiles, while relatively few products were observed. In addition, the NHG or NHA radical most likely to be formed would be expected to rapidly eliminate NO (62). (ii) A two-electron oxidation of one substrate molecule produces a highly reactive transient species (X in Scheme II), which, upon escape from the active site, reacts rapidly with a second substrate molecule.

The obvious candidate is the nitrosoamidine (Table I), formed by dehydrogenation, which could react with a second substrate molecule to give the *N*-nitroso product and a molecule of cyanamide or CN-orn. This was postulated as an intermediate in the peroxide-shunt mechanism of NOS by Clague *et al.* (20) but dismissed since it does not account for incorporation of ^{18}O into the citrulline product; in our case, no citrulline is observed and so we have no such grounds. However, it is not obvious why this reaction would be so specific, since expulsion of NO or NO^- and formation of urea/citrulline as well as cyanamide/CN-orn might be reasonably expected to compete. (iii) Two-electron oxidation of the first substrate by the heme results in the formation of cyanamide or CN-orn and HNO, which efficiently recombines with the ferric heme to form a "heme-NO" nitrosating intermediate. This, or a related complex, may be the nitrosating intermediate (X in Scheme II) responsible for reaction with a second substrate molecule. Neither of the latter two proposals account for the 1:1 stoichiometry observed between NHG and H_2O_2. However, we note that stoichiometry experiments involving peroxide oxidation are easily in error due to the potential catalase-like activity of the mutants, or because of lost oxidation equivalents.

Several chemical models capable of guanidine oxidation have been characterized (63). Some chemical agents, such as $Pb(OAc)_4$, oxidize *N*-hydroxyguanidino compounds to produce NO, while others, such as Ag_2CO_3, produce the metastable HNO, detected as N_2O. Each of these produce the cyanamide functionality rather than the urea (64). However, peracid oxidation of *N*-hydroxyguanidines is reported to give the urea equivalent and HNO (65) and the short-lived NHG radical also rapidly eliminates NO (62). While the chemical nature of these oxidants, and thus their molecular mechanisms, are very different from an enzymatic active site, the reactions catalyzed are of interest in establishing the various alternative chemistries. The oxidation of *N*-hydroxyguanidines by other heme enzymes such as horseradish peroxidase (66) and microsomal cytochrome P_{450} has also been reported to produce NO and the corresponding nitriles or urea compounds, although the superoxide anion, derived from P_{450}-catalyzed O_2 reduction, has been proposed to play a major role in this case (67–69). Thus, the H_2O_2-dependent chemistry catalyzed by R48A is clearly distinct from that previously reported for NOS, chemical model systems or indeed those reactions catalyzed by other heme systems.

Acknowledgements—The nitrophorin-1 expression vector was a kind gift from Prof. Ann Walker. We also thank Dr. Philip Dawson, Prof. John Groves, Prof, T. L. Poulos, Dr. Duncan McRee, Dr. John Murphy, Dr. Christoph Schalley, Dr. Pamela Williams, and Dr. Sheri Wilcox for valuable discussions.

REFERENCES

1. Anni, H., and Yonetani, T. (1992) *Met. Ions Biol. Syst.* **28,** 219–241
2. Dunford, H. B. (1982) *Adv. Inorg. Biochem.* **4,** 41–68
3. Ortiz de Montellano, P. R. (1987) *Acc. Chem. Res.* **20,** 289–294
4. Sono, M., Roach, M. P., Coulter, E. D., and Dawson, J. H. (1996) *Chem. Rev.* **96,** 2841–2887
5. Poulos, T. L., and Finzel, B. C. (1984) *Peptide Protein Rev.* **4,** 115–171
6. Finzel, B. C., Poulos, T. L., and Kraut, J. (1984) *J. Biol. Chem.* **259,** 13027–13036
7. Dawson, J. H. (1988) *Science* **240,** 433–439
8. Ortiz de Montellano, P. R. (1992) *Annu. Rev. Pharmacol. Toxicol.* **32,** 89–107
9. Groves, J. T. (1985) *J. Chem. Educ.* **62,** 928–931
10. Bruice, T. C. (1991) *Acc. Chem. Res.* **24,** 243–249
11. Stern, M. K., and Groves, J. T. (1992) in *Manganese Redox Enzymes* (Pecoraro,

V. L., ed) pp. 233–259, VCH, New York
12. Traylor, T. G., Mincey, T., Berzinis, A., and White, D. (1982) in *Oxidases and Related Redox Systems* (King, T. E., Mason, H. S., and Morrison, M., eds) Vol. 3, pp. 565–571, Pergamon, New York
13. Ignarro, L. J., Buga, G. M., Wood, K. S., Byrns, R. E., and Chaudhuri, G. (1987) *Proc. Natl. Acad. Sci. U. S. A.* **84,** 9265–9269
14. Palmer, R. M. J., Ferrige, A. G., and Moncada, S. (1987) *Nature* **327,** 524–526
15. Marletta, M. A. (1993) *J. Biol. Chem.* **268,** 12231–12234
16. Pufahl, R. A., and Marletta, M. A. (1993) *Biochem. Biophys. Res. Commun.* **193,** 963–970
17. Crane, B. R., Arvai, A. S., Ghosh, D. K., Wu, C., Getzoff, E. D., Stuehr, D. J., and Tainer, J. A. (1998) *Science* **279,** 2121–2126
18. Abu-Soud, H. M., Presta, A., Mayer, B., and Stuehr, D. J. (1997) *Biochemistry* **36,** 10811–10816
19. Pufahl, R. A., Wishnok, J. S., and Marletta, M. A. (1995) *Biochemistry* **34,** 1930–1941
20. Clague, M. J., Wishnok, J. S., and Marletta, M. A. (1997) *Biochemistry* **36,** 14465–14473
21. Rusche, K. M., Spiering, M. M., and Marletta, M. A. (1998) *Biochemistry* **37,** 15503–15512
22. Toney, M. D., and Kirsch, J. F. (1989) *Science* **243,** 1485–1488
23. McRee, D. E., Jensen, G. M., Fitzgerald, M. M., Siegel, H. A., and Goodin, D. B. (1994) *Proc. Natl. Acad. Sci. U. S. A.* **91,** 12847–12851
24. Denblaauwen, T., Vandekamp, M., and Canters, G. W. (1991) *J. Am. Chem. Soc.* **113,** 5050–5052
25. Barrick, D. (1994) *Biochemistry* **33,** 6546–6554
26. Fitzgerald, M. M., Churchill, M. J., McRee, D. E., and Goodin, D. B. (1994) *Biochemistry* **33,** 3807–3818
27. Musah, R. A., and Goodin, D. B. (1997) *Biochemistry* **36,** 11665–11674
28. Howard, A. J., Nielson, C., and Xuong, N. H. (1985) *Methods Enzymol.* **114,** 452–472
29. McRee, D. E. (1992) *J. Mol. Graphics* **10,** 44–46
30. Navaza, J. (1994) *Acta Crystallogr.* **50,** 157–163
31. Sheldrick, G. M. (1997) *Methods Enzymol.* **276,** 628–641
32. Baker, M. D., Mohammed, H. Y., and Veening, H. (1981) *Anal. Chem.* **53,** 1658–1662
33. Bidlingmeyer, B. A., Cohen, S. A., and Tarvin, T. L. (1984) *J. Chromatogr.* **336,** 93–104
34. Molnar-Perl, I. (1994) *J. Chromatogr.* **661,** 43–50
35. Green, L. C., Wagner, D. A., Glogowski, J., Skipper, P. L., Wishnok, J. S., and Tannenbaum, S. R. (1982) *Anal. Biochem.* **126,** 131–138
36. Vitello, L. B., Erman, J. E., Miller, M. A., Wang, J., and Kraut, J. (1993) *Biochemistry* **32,** 9807–9818
37. Miller, M. A., Mauro, J. M., Smulevich, G., Coletta, M., Kraut, J., and Traylor, T. G. (1990) *Biochemistry* **29,** 9978–9988
38. Eriksson, A. E., Baase, W. A., Wozniak, J. A., and Matthews, B. W. (1992) *Nature* **355,** 371–373
39. Musah, R. A., Jensen, G. M., Rosenfeld, R. J., Bunte, S. W., McRee, D. E., and Goodin, D. B. (1997) *J. Am. Chem. Soc.* **119,** 9083–9084
40. Goodin, D. B., and McRee, D. E. (1993) *Biochemistry* **32,** 3313–3324
41. Caminiti, R., Pieretti, A., Bencivenni, L., Ramondo, F., and Sanna, N. (1996) *J. Phys. Chem.* **100,** 10928–10935
42. Sapse, A. M., Herzig, L., and Snyder, G. (1981) *Cancer Res.* **41,** 1824–1828
43. Kneip, T. J., Daisey, J. M., Solomon, J. J., and Hershman, R. J. (1983) *Science* **221,** 1045–1047
44. Greenberg, S. S., Xie, J., Spitzer, J. J., Wang, J., Lancaster, J., Grisham, M. B., Powers, D. R., and Giles, T. D. (1995) *Life Sci.* **57,** 1949–1961
45. Bazylinski, D. A., and Hollocher, T. C. (1985) *J. Am. Chem. Soc.* **107,** 7982–7986
46. Andersen, J. F., Champagne, D. E., Weichsel, A., Ribeiro, J. M. C., Balfour, C. A., Dress, V., and Montfort, W. R. (1997) *Biochemistry* **36,** 4423–4428
47. Glaser, R., Murmann, R. K., and Barnes, C. L. (1996) *J. Org. Chem.* **61,** 1047–1058
48. Southan, G. J., and Srinivasan, A. (1998) *Nitric Oxide* **2,** 270–286
49. Crane, B. R., Arvai, A. S., Gachhui, R., Wu, C., Ghosh, D. K., Getzoff, E. D., Stuehr, D. J., and Tainer, J. A. (1997) *Science* **278,** 425–431
50. Raman, C. S., Li, H., Martasek, P., Kral, V., Masters, B. S. S., and Poulos, T. L. (1998) *Cell* **95,** 939–950
51. Poulos, T. L. (1988) *Adv. Inorg. Biochem.* **7,** 1–36
52. Wilcox, S. K., Putnam, C. D., Sastry, M., Blankenship, J., Chazin, W. J., McRee, D. E., and Goodin, D. B. (1998) *Biochemistry* **37,** 16853–16862
53. Miller, V. P., DePillis, G. D., Ferrer, J. C., Grant, M. A., and Ortiz de Montellano, P. R. (1992) *J. Biol. Chem.* **267,** 8936–8942
54. Halpert, J. R., and He, Y. A. (1993) *J. Biol. Chem.* **268,** 4453–4457
55. Atkins, W. M., and Sligar, S. G. (1989) *J. Am. Chem. Soc.* **111,** 2715
56. Ozaki, S., Matsui, T., and Watanabe, Y. (1997) *J. Am. Chem. Soc.* **119,** 6666–6667
57. Ozaki, S., Matsui, T., and Watanabe, Y. (1996) *J. Am. Chem. Soc.* **118,** 9784–9785
58. Erman, J. E., and Vitello, L. B. (1998) *J. Biochem. Mol. Biol.* **31,** 307–327
59. Poulos, T. L., and Raag, R. (1992) *FASEB J.* **6,** 674–679
60. Wang, J., Stuehr, D. J., Ikeda-Saito, M., and Rousseau, D. L. (1993) *J. Biol. Chem.* **268,** 22255–22268
61. Sivaraja, M., Goodin, D. B., Smith, M., and Hoffman, B. M. (1989) *Science* **245,** 738–740
62. Everett, S. A., Patel, K. B., Dennis, M. F., Smith, K. A., Stratford, M. R. L., and Wardman, P. (1998) *Free Radical Biol. Med.* **24,** 1–10
63. Fukuto, J. M. (1996) *Methods Enzymol.* **268,** 365–375
64. Fukuto, J. M., Wallace, G. C., Hszieh, R., and Chaudhuri, G. (1992) *Biochem. Pharm.* **43,** 607–613
65. Fukuto, J. M., Stuehr, D. J., Feldman, P. L., Bova, M. P., and Wong, P. (1993) *J. Med. Chem.* **36,** 2666–2670
66. Boucher, J. L., Genet, A., Vadon, S., Delaforge, M., and Mansuy, D. (1992) *Biochem. Biophys. Res. Commun.* **184,** 1158–1164
67. Jousserandot, A., Boucher, J.-L., Henry, Y., Niklaus, B., Clement, B., and Mansuy, D. (1998) *Biochemistry* **37,** 17179–17191
68. Mansuy, D., Boucher, J.-L., and Clement, B. (1995) *Biochimie* **77,** 661–667
69. Sennequier, N., Boucher, J.-L., Battioni, P., and Mansuy, D. (1995) *Tetrahedron Lett.* **36,** 6059–6062